Progress In Electromagnetics Research, PIER 84, 93–104, 2008

SENSITIVITY OF TRANSFORMATION CLOAK IN ENGINEERING

J. J. Zhang, Y. Luo, H. S. Chen[†], and B.-I. Wu[‡]

The Electromagnetics Academy at Zhejiang University
Zhejiang University
Hangzhou 310058, P. R. China

Abstract—The sensitivity of cylindrical and spherical transformation cloak to several factors has been carefully studied in this paper. We find that the performance of the transformation cloak is quite sensitive to the crevice in the shell. When an obstacle is not completely wrapped inside the cloaking shell, noticeable scattering will be induced outside. It is also shown that if the shape of the cloak is changed in certain ways while the material parameters remain the same, the backward scattering is still zero. In addition, the combination of parts of cylindrical cloak can only achieve perfect invisibility in one direction, while combining the cylindrical cloak with two halves of spherical cloak can still make a perfect 3-dimensional (3D) invisible cloak. The findings are verified with finite element based simulations as well as theoretical calculations. Our discussion results are valuable to the implementation of cloak in engineering.

1. INTRODUCTION

Recently, there is an increasing interest on hiding objects from EM detection with cloaking devices [1–17]. Pendry et al. [1] suggested that with metamaterial, the detecting wave can be bent around the obstacle without touching it. Schurig et al. verified the idea by calculating the material properties associated with a coordinate transformation and used these properties to perform ray tracing [2]. Full wave numerical simulations on cylindrical cloaking were presented by Cummer, who also proposed the idea of using reduced parameters to simplify the

[†] Author to whom correspondence should be addressed, electronic email: chenhs@ewt.mit.edu
[‡] The third and fourth authors are also with Research Laboratory of Electronics, Massachusetts Institute of Technology, Cambridge, Massachusetts 02139, USA.

cloaking fabrication process [3]. The experimental demonstration of circular cylinder cloaks is reported afterwards [4], which attract more exploration on the topic of invisible cloak regarding the practical applications [5, 6]. Up to now, most of the theoretical discussion and experimental realization of cloak are focused on cylindrical and spherical cloaks, which is due to the relative simplicity of their parameters [1–10]. However, in engineering, some non-ideal factors in the fabrication process will sometimes affect the shape of the cloak, or even result in some crevices in the cloaking shell. In this paper, we discussed the sensitivity of the cloak to these non-ideal factors. It is found that the performance of the cloak is very sensitive to the crevice in the shell. Even a small slit will cause a noticeable scattering outside. We have also shown that a cloak with perfect material parameters but changed shape has zero backward scattering. For some special cases, it can even realize perfect invisibility in one direction. Finally, the possibility of implementing cloaking of other shapes with segmented pieces of ideal 2D and 3D cloaks is discussed. It is found that combining parts of 2D cloaks cannot achieve perfect invisibility. Even with properly combination method, we can only observe the invisible behavior when the cloak is illuminated in one specific direction. In contrast, 3D perfect cloaking can be easily realized by combining a finite cylindrical cloak with two halves of spherical cloaks. Numerical simulations are performed to examine all the findings, showing the validity of results to the implementation of cloak in engineering.

2. 2D IMPERFECT CLOAK CREATED WITH SEGMENTS OF SPHERICAL CLOAKS

Let us start with scrutinizing the scattering behavior of the two cloak parts separated by a slit with numerical simulation based on finite element method. Fig. 1 describes the field distribution of cloak parts in four cases. In Fig. 1(a), an ideal cylindrical cloak with the following material parameters is illuminated by a TE plane wave [2, 17]:

$$\varepsilon_\rho = \mu_\rho = \frac{f(\rho)}{\rho f'(\rho)}, \quad \varepsilon_\varphi = \mu_\varphi = \frac{\rho f'(\rho)}{f(\rho)}, \quad \varepsilon_z = \mu_z = \frac{f'(\rho) f(\rho)}{\rho} \quad (1)$$

where $f(\rho)$ is the transformation function with $f(R_1) = 0$, $f(R_2) = R_2$. R_1 and R_2 represent the inner and outer radius of the cloak, respectively. For some special cases, we might not be able to completely wrap an object inside a closed shell. Therefore, it is necessary to estimate how a crevice in a cloak shell affects the cloaking performance. We first remove half of the cloak shell and calculate the field distribution by using finite element method (FEM), which

is shown in Fig. 1(b). The simulated results indicate large forward scattering is caused and a shadow can be observed behind the half cloak shell. Adding the other half of the cloak but still leaving a slit between the two halves will not improve the scattering behavior, which can be seen in Fig. 1(c). Moving these two parts far apart can cause an even larger scattering, as depicted in Fig. 1(d). The above results clearly show that chapped cloak can not make the object inside invisible, even if the rift is very small.

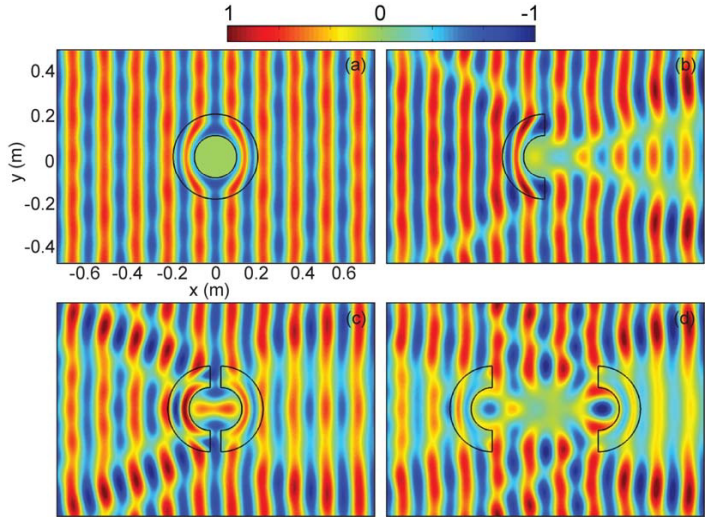

Figure 1. (Color online) The electric field distribution of TE wave illuminated 2D cloaks in four different cases: (a) the ideal cloak (b) half of the cloak (c) two equal halves of the cloak with a small slit which separates the two parts (d) two separated equal halves of the cloak with a distance apart.

Since perfect invisibility cannot be achieved when there is a crevice in the cloak, we next discuss the possibility of improving the performance of this chapped cloak. For the purpose of wrapping the object completely, we add two slabs to the separated cloak shells to make a reshaped cloak. The relative permittivity and permeability tensors of the upper slab are

$$\varepsilon_x = \mu_x = g'(y), \quad \varepsilon_y = \mu_y = \frac{1}{g'(y)}, \quad \varepsilon_z = \mu_z = g'(y) \tag{2}$$

In order to make the connected boundary perfect matched, here linear transformation function is selected as $g(t) = f(t)$ for $R_1 < t < R_2$. The

parameters for the nether slab can be similarly achieved. We simulate both TE polarized incidence and TM polarized incidence cases in two orthogonal directions. The results shown in Fig. 2 indicate that only when a TM polarized plane wave is incident along x direction, the scattering outside is exactly zero. Thereby, only imperfect 2D cloak which can realize invisibility in one certain direction can be achieved by combining the two pieces of cylindrical cloak.

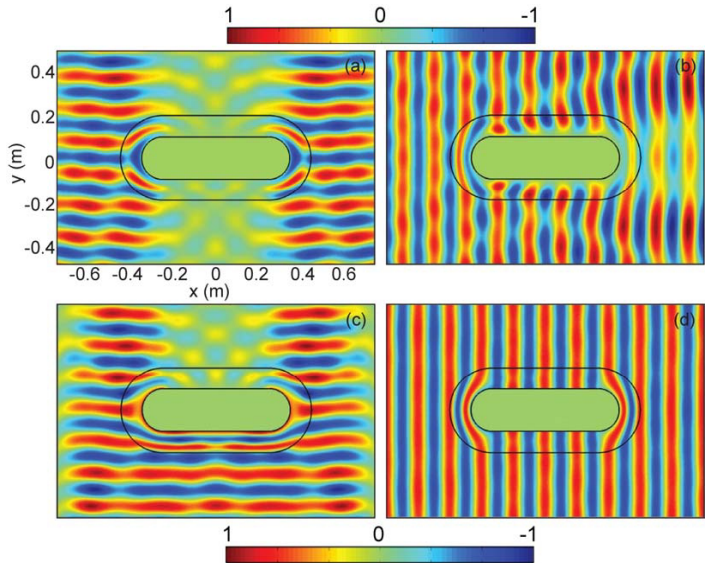

Figure 2. (Color online) The electric field distribution of a 2D cloak created by combining two separated halves of the circular cylindrical cloak with metamaterial slabs. (a) vertical TE wave illumination (b) horizontal TE wave illumination (c) vertical TM wave illumination (d) horizontal TM wave illumination.

Our next step is to analyze how sensitive the cloak is to the shape, since a cloak fabricated in engineering might not always be realized with the perfect profile. In order to simply the discussion, we first segment the cloak shell into two unequal parts with material parameters unchanged and then combine two parts which are smaller than half together to make a reshaped cloak, as shown in Fig. 3(a) and (b). It is found that the backward scattering is always zero, which indicates that from monostatic detection, an obstacle inside the cloak is still invisible to the observer. In addition, it can be seen that under a vertical illumination (Fig. 3(a)), perfect invisibility can be achieved while in horizontal illumination case (Fig. 3(b)),

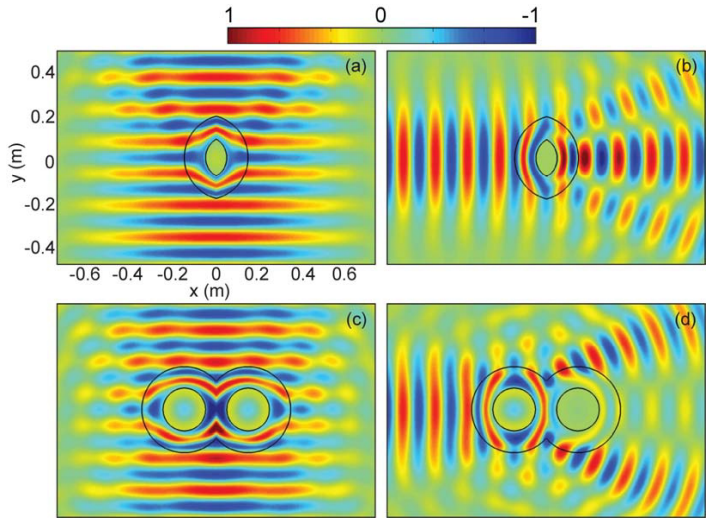

Figure 3. (Color online) The electric field distribution of TE wave illuminated cloaks created by combining two parts of the ideal cylindrical cloak (a) the 'one cell' reshaped cloak under the vertical illumination (b) the 'one cell' reshaped cloak under the horizontal illumination (c) the 'two cell' reshaped cloak under the vertical illumination (d) the 'two cell' reshaped cloak under the horizontal illumination.

strong forward scattering is induced. This phenomenon is not difficult to understand. We know that the inner boundary of the original cylindrical cloak is mapped from a point. The truncation of the inner boundary will disturb the paths of the rays when the wave is horizontally incident, which will cause scattering as a result. This can also be confirmed by another case, where two parts of the cloak larger than half are combined to form a "two cell" reshaped cloak. In this case, the light paths in the central region will be disturbed in both vertical and horizontal illumination conditions. Thereby, large forward scattering can be observed in both Figs. 3(b) and (d), although the backward scattering remains zero for both cases. This result indicates perfect invisibility cannot be achieved in all the cases. What should be noticed is that the field inside the core of the shell is still zero, though here small electric field inside the cloak can be observed in Fig. 3, which is due to the limited precision of the numerical simulation (It has already been demonstrated that even a small perturbation at the boundary can introduce EM field to the inside region of the cloak).

The zero inner field indicates that the scattering is caused by the coating itself. Therefore, the observer outside cannot see what exactly the obstacle is inside the coating, since whatever the obstacle is, the scattered field outside is always the same.

3. 3D PERFECT CLOAK CREATED WITH SEGMENTS OF CYLINDRICAL AND SPHERICAL CLOAKS

We will show in this section that perfect invisibility can be achieved by a proper combination of two pieces of slit spherical cloak, the process of which is shown in Fig. 4. We consider a 3D reshaped cloak by adding a truncated cylindrical cloak (with length L along the axial direction) and two half spherical shells (whose centers are located at (0, 0, $L/2$) and (0, 0, $-L/2$) respectively) together. Suppose the material parameters of the truncated cylinder take exactly the same forms of Eqs. (1), and the relative permittivity and permeability tensors of the upper semi-sphere are expressed as:

$$\varepsilon_r = \mu_r = \frac{h^2(r_1)}{r_1^2 h'(r_1)}, \qquad \varepsilon_\theta = \mu_\theta = \varepsilon_\varphi = \mu_\varphi = h'(r_1). \tag{3a}$$

while the parameters of the bottom semi-sphere are

$$\varepsilon_r = \mu_r = \frac{h^2(r_2)}{r_2^2 h'(r_2)}, \qquad \varepsilon_\theta = \mu_\theta = \varepsilon_\varphi = \mu_\varphi = h'(r_2). \tag{3b}$$

where $r_1 = \sqrt{x^2 + y^2 + (z - L/2)^2}$ and $r_2 = \sqrt{x^2 + y^2 + (z + L/2)^2}$. $h(t)$ is the transformation function with $h(R_1) = 0$ and $h(R_2) = R_2$. R_1 and R_2 represent the inner and outer radius of the cloak, respectively. Since at the interior boundary of the cloaking $f(R_1) = 0$

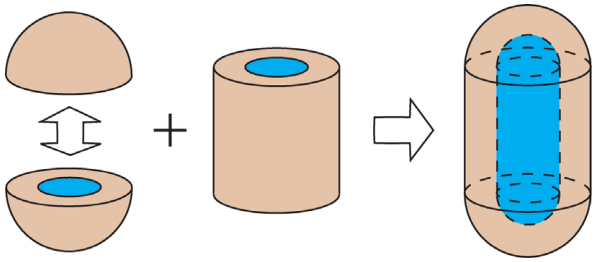

Figure 4. Schematic for the process of combining truncated cylindrical cloak and two halves of spherical cloak.

and $h(R_1) = 0$, it can be demonstrated that the fields scattered by this boundary as well as the fields penetrating inside the cloaking are exactly equal to zero [9]. Meanwhile at the outer boundary of the cloaking $f(R_2) = R_2$ and $h(R_2) = R_2$, which indicates that the reshaped cloaking is perfectly matched to the background. Therefore, the scattered power outside could only be caused at the connected boundary. The transformation function $h(t)$ is hence chosen to be $f(t)$ for $R_1 < t < R_2$ in order to make the fields matched at the connected boundary. The scattering characteristics of this reshaped cloaking can be further examined by analytically calculating the field distribution [18–28]. Following the same steps of [7] and [9], we decompose the fields into TE and TM modes by introducing vector potentials $\bar{A}_{\mathrm{TM}}$ and $\bar{A}_{\mathrm{TE}}$, respectively [9]:

$$B_{\mathrm{TM}} = \nabla \times \left(\bar{A}_{\mathrm{TM}}\right) \tag{4a}$$

$$D_{\mathrm{TM}} = \frac{i}{\omega}\left[\nabla \times \left(\bar{\bar{\mu}}^{-1} \cdot \nabla \times \left(\bar{A}_{\mathrm{TM}}\right)\right)\right] \tag{4b}$$

$$D_{\mathrm{TE}} = -\nabla \times \left(\bar{A}_{\mathrm{TE}}\right) \tag{4c}$$

$$B_{\mathrm{TE}} = \frac{i}{\omega}\left[\nabla \times \left(\bar{\bar{\varepsilon}}^{-1} \cdot \nabla \times \left(\bar{A}_{\mathrm{TE}}\right)\right)\right] \tag{4d}$$

Let $\cos(\theta_1) = (z - L/2)/r_1$, $\cos(\theta_2) = (z + L/2)/r_2$, then we can obtain the scalar potentials in the truncated cylindrical cloak layer, the top semi-spherical layer and the bottom semi-spherical layer to be of the following forms, respectively:

$$\begin{aligned}
\bar{A}^{\mathrm{cly}}_{\mathrm{TM}} &= \hat{z}\int_{\Gamma^{\mathrm{cly}}_{\mathrm{TM}}} dk_z \sum_{n\in\Im^{\mathrm{cly}}_{\mathrm{TM}}} a^{\mathrm{TM}}_{k_z,n} J_n\left(\sqrt{k_0^2 - k_z^2}\, f(\rho)\right) e^{in\varphi + ik_z z} \\
\bar{A}^{\mathrm{cly}}_{\mathrm{TE}} &= \hat{z}\int_{\Gamma^{\mathrm{cly}}_{\mathrm{TE}}} dk_z \sum_{n\in\Im^{\mathrm{cly}}_{\mathrm{TE}}} a^{\mathrm{TE}}_{k_z,n} J_n\left(\sqrt{k_0^2 - k_z^2}\, f(\rho)\right) e^{in\varphi + ik_z z}
\end{aligned} \tag{5a}$$

$$\begin{aligned}
\bar{A}^{\mathrm{up}}_{\mathrm{TM}} &= \left(\hat{r}_1 h'(r_1)\cos\theta_1 - \hat{\theta}_1 \frac{h(r_1)}{r_1}\sin\theta_1\right)\int_{\Lambda^{\mathrm{up}}_{\mathrm{TM}}} d\nu \\
&\quad \sum_{n\in\Re^{\mathrm{up}}_{\mathrm{TM}}} b^{\mathrm{TM}}_{\nu,n} j_\nu\left(k_0 h(r_1)\right) P^n_\nu(\cos\theta_1)\, e^{in\varphi} \\
\bar{A}^{\mathrm{up}}_{\mathrm{TE}} &= \left(\hat{r}_1 h'(r_1)\cos\theta_1 - \hat{\theta}_1 \frac{h(r_1)}{r_1}\sin\theta_1\right)\int_{\Lambda^{\mathrm{up}}_{\mathrm{TE}}} d\nu \\
&\quad \sum_{n\in\Re^{\mathrm{up}}_{\mathrm{TE}}} b^{\mathrm{TE}}_{\nu,n} j_\nu\left(k_0 h(r_1)\right) P^n_\nu(\cos\theta_1)\, e^{in\varphi}
\end{aligned} \tag{5b}$$

$$\bar{A}_{\mathrm{TM}}^{\mathrm{bot}} = \left(\hat{r}_2 h'(r_2)\cos\theta_2 - \hat{\theta}_2 \frac{h(r_2)}{r_2}\sin\theta_2\right) \int_{\Omega_{\mathrm{TM}}^{\mathrm{bot}}} d\nu \sum_{n\in\aleph_{\mathrm{TM}}^{\mathrm{bot}}} c_{\nu,n}^{\mathrm{TM}} j_\nu\left(k_0 h(r_2)\right) P_\nu^n(\cos\theta_2)\, e^{in\varphi}$$
$$\bar{A}_{\mathrm{TE}}^{\mathrm{bot}} = \left(\hat{r}_2 h'(r_2)\cos\theta_2 - \hat{\theta}_2 \frac{h(r_2)}{r_2}\sin\theta_2\right) \int_{\Omega_{\mathrm{TM}}^{\mathrm{bot}}} d\nu \sum_{n\in\aleph_{\mathrm{TM}}^{\mathrm{bot}}} c_{\nu,n}^{\mathrm{TE}} j_\nu\left(k_0 h(r_2)\right) P_\nu^n(\cos\theta_2)\, e^{in\varphi} \quad (5c)$$

where J_n, j_ν, and P_ν^n are n-th order Bessel function, ν-th order spherical Bessel function, and ν-th order associated Legendre polynomials of degree n. All the unknown coefficients $a_{kz,n}^{\mathrm{TM}}$, $a_{kz,n}^{\mathrm{TE}}$, $b_{\nu,n}^{\mathrm{TM}}$, $b_{\nu,n}^{\mathrm{TE}}$, $c_{\nu,n}^{\mathrm{TM}}$, and $c_{\nu,n}^{\mathrm{TE}}$ as well as the admissible value of separation parameters k_z, ν, and n can be determined by applying boundary conditions. Finally, all the components of the fields can be obtained by substituting Eqs. (5) into Eqs. (4). Fig. 5 shows the analytically calculated field distribution of a 3D cloak under the TE polarized illumination of three different directions. It can be seen that the waves are guided around the cloak cover without inducing any scattering, which indicates an omni-directional perfect invisible capability.

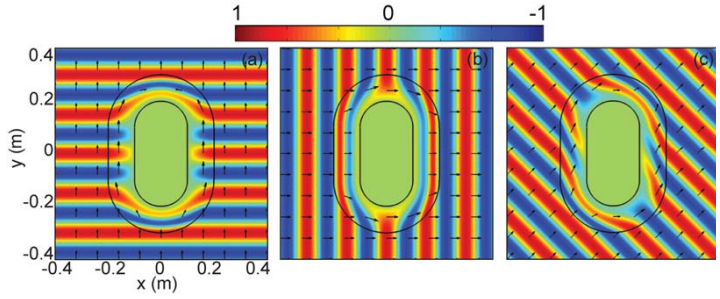

Figure 5. (Color online) The electric field distribution of a 3d cloak created by combining two halves of the spherical cloak with cylindrical cloak. (a) vertical TE wave illumination (b) horizontal TE wave illumination (c) oblique TE wave illumination.

4. DISCUSSION

One point that should be taken into consideration when we combine the cloak pieces to make a reshaped cloak is the continuity of fields at

the connected boundary. Take the case shown in Fig. 2 as an example. As the parameters are all matched at the connected boundaries, a plane surface which connects the centers of the two halves of the cylindrical shell is mapped to the inner boundary of the cloak while the outer boundary is matched to free space. And it's easy to understand that only in the direction that is parallel to the original plane, the incident wave can be guided smoothly around the inner region. However, in the 3D case as depicted in Fig. 4, the inner boundary of the cloak is transformed from a straight line connecting the centers of the two half spheres. That is why the inside region is invisible no matter observed in which direction.

We already know that the invisibility of the cylindrical cloak desires the infinity in the axial direction. Adding two half spherical cloak shells to the truncated ends provides a solution to the problem of inducing scattering. Therefore, we can choose the length of the cylindrical cloak as we need and 'seal' the open ends simply with the segments of the cloak of other shapes. This design scheme is applicable in many cases where we need to conceal some objects with long cylindrical contours.

5. CONCLUSION

How the transformation cloak with ideal parameters reacts to some disturbance factors in engineering is discussed in this paper. It is shown with numerical simulations that the performance of cloak will be deteriorated when a crevice appears in the cloak. In 2D case, combining the two separated parts with appropriately designed metamaterial slabs will only yield an imperfect cloak which can realize invisibility in one direction, while in 3D case, connecting two half spheres with a truncated cylindrical cloak can achieve perfect invisible behavior. The sensitivity of 2D cloak to the shape is also studied with two specific cases.

ACKNOWLEDGMENT

This work is sponsored by the Chinese National Science Foundation under Grant Nos. 60531020 and 60671003, the NCET-07-0750, the ONR under Contract No. N00014-06-1-0001, the Department of the Air Force under Air Force Contract No. F19628-00-C-0002, and the excellent doctoral thesis foundation of Zhejiang University (No. 08009A).

REFERENCES

1. Pendry, J. B., D. Schurig, and D. R. Smith, "Controlling electromagnetic fields," *Science*, Vol. 312, 1780, 2006.
2. Schurig, D., J. B. Pendry, and D. R. Smith, "Calculation of material properties and ray tracing in transformation media," *Opt. Express*, Vol. 14, 9794, 2006.
3. Cummer, S. A., B.-I. Popa, D. Schurig, D. R. Smith, and J. B. Pendry, "Full-wave simulations of electromagnetic cloaking structures," *Phys. Rev. E*, Vol. 74, 036621, 2006.
4. Schurig, D., J. J. Mock, B. J. Justice, S. A. Cummer, J. B. Pendry, A. F. Starr, and D. R. Smith, "Metamaterial electromagnetic cloak at microwave frequencies," *Science*, Vol. 314, 977, 2006.
5. Cai, W., U. K. Chettiar, A. V. Kildishev, and V. M. Shalaev, "Optical cloaking with metamaterials," *Nature Photon.*, Vol. 1, 224, 2007.
6. Zhang, J., J. Huangfu, Y. Luo, H. Chen, J. A. Kong, and B.-I. Wu, "Cloak for multilayered and gradually changing media," *Phys. Rev. B*, Vol. 77, 035116, 2008.
7. Chen, H., B.-I. Wu, B. Zhang, and J. A. Kong, "Electromagnetic wave interactions with a metamaterial cloak," *Phys. Rev. Letts.*, Vol. 99, 063903, 2007.
8. Zolla, F., S. Guenneau, A. Nicolet, and J. B. Pendry, "Electromagnetic analysis of cylindrical invisibility cloaks and the mirage effect," *Opt. Lett.*, Vol. 32, 1069, 2007.
9. Luo, Y., J. Zhang, L. Ran, H. Chen, and J. A. Kong, "Design and analytical full-wave validation of the invisibility cloaks, concentrators, and field rotators created with a general class of transformations," *Phys. Rev. B*, Vol. 77, 125127, 2008.
10. Weder, R., "A rigorous analysis of high-order electromagnetic invisibility cloaks," *J. Phys. A: Math. Theor.*, Vol. 41, 065207, 2008.
11. Xi, S., H. Chen, B.-I. Wu, B. Zhang, J. Huangfu, D. Wang, and J. A. Kong, "Effects of different transformations on the performance ofcylindrical cloaks," *Journal of Electromagnetic Waves and Applications*, Vol. 22, 1489, 2008.
12. Rahm, M., D. Schurig, D. A. Roberts, S. A. Cummer, D. R. Smith, and J. B. Pendry, "Design of electromagnetic cloaks and concentrators using form-invariant coordinate transformations of Maxwell's equations," *Photonics Nanostruct. Fundam. Appl.*, Vol. 6, 87, 2008.

13. Ma, H., S. Qu, Z. Xu, J. Zhang, B. Chen, and J. Wang, "Material parameter equation for elliptical cylindrical cloaks," *Phys. Rev. A*, Vol. 77, 013825, 2008.
14. Kwon, D.-H. and D. H. Werner, "Two-dimensional electromagnetic cloak having a uniform thickness for elliptic cylindrical regions," *Appl. Phys. Letts.*, Vol. 92, 113502, 2008.
15. Kwon, D.-H. and D. H. Werner, "Two-dimensional eccentric elliptic electromagnetic cloaks," *Appl. Phys. Letts.*, Vol. 92, 013505, 2008.
16. Zhang, J., Y. Luo, S. Xi, H. S. Chen, L. Ran, B.-I. Wu, and J. A. Kong, "Directive emission obtained by coordinate transformation," *Progress In Electromagnetics Research*, PIER 81, 437, 2008.
17. Cai, W., U. K. Chettiar, A. V. Kildishev, and V. M. Shalaev, "Nonmagnetic cloak with minimized scattering," *Appl. Phys. Lett.*, Vol. 91, 111105, 2007.
18. Du, P., B. Wang, H. Li, and G. Zheng, "Scattering analysis of large-scale periodic structures using the sub-entire domain basis function method and characteristic function method," *Journal of Electromagnetic Waves and Applications*, Vol. 21, 2085, 2007.
19. Abd-El-Raouf, H. and R. Mittra, "Scattering analysis of dielectric coated cones," *Journal of Electromagnetic Waves and Applications*, Vol. 21, 1857, 2007.
20. Hady, L. K. and A. A. Kishk, "Electromagnetic scattering from conducting circular cylinder coated by meta-materials and loaded with helical strips under oblique incidence," *Progress In Electromagnetics Research B*, Vol. 3, 189, 2008.
21. Valagiannopoulos, C. A., "Electromagnetic scattering from two eccentric metamaterial cylinders with frequency-dependent permittivities differing slightly each other," *Progress In Electromagnetics Research B*, Vol. 3, 23, 2008.
22. Li, X.-F., Y.-J. Xie, and R. Yang, "High-frequency method analysis on scattering from homogenous dielectric objects with electrically large size in half space," *Progress In Electromagnetics Research B*, Vol. 1, 177, 2008.
23. Illahi, A., M. Afzaal, and Q. A. Naqvi, "Scattering of dipole field by a perfect electromagnetic conductor cylinder," *Progress In Electromagnetics Research Letters*, Vol. 4, 43, 2008.
24. Sun, X. and H. Ha, "Light scattering by large hexagonal column with multiple densely packed inclusions," *Progress In Electromagnetics Research Letters*, Vol. 3, 105, 2008.

25. Kokkorakis, G. C., "Scalar equations for scattering by rotationally symmetric radially inhomogeneous anisotropic sphere," *Progress In Electromagnetics Research Letters*, Vol. 3, 179, 2008.
26. Li, Y.-L., J.-Y. Huang, M.-J. Wang, and J. Zhang, "Scattering field for the ellipsoidal targets irradiated by an electromagnetic wave with arbitrary polarizing and propagating direction," *Progress In Electromagnetics Research Letters*, Vol. 1, 221, 2008.
27. Li, Y., J. Huang, and M. Wang, "Scattering cross section for airborne and its application," *Journal of Electromagnetic Waves and Applications*, Vol. 21, 2341, 2007.
28. Choi, S., D. Seo, and N. Myung, "Scattering analysis of open-ended cavity with inner object," *Journal of Electromagnetic Waves and Applications*, Vol. 21, 1689, 2007.